ASEAN
Journal of Scientific and Technological Reports
Online ISSN:2773-8752

Research article

Detection of COVID-19, Pneumonia, and Tuberculosis Using Convolutional Neural Networks and Ensemble of Deep Learning Architectures

Rituraj Jain[1*], Simon Kasahun Bekele[2], Damodharan Palaniappan[3], Kumar Parmar[4], Ramesh Babu P[5], and Anandkumar M. Trivedi[6]

[1] Department of Information Technology, Marwadi University, Rajkot, Gujarat, India
[2] Engineer, Cooperative Bank of Oromia, Addis Ababa, Ethiopia
[3] Department of Information Technology, Marwadi University, Rajkot, Gujarat, India
[4] Department of Information Technology, Marwadi University, Rajkot, Gujarat, India
[5] Department of CSE, KL Education Foundation, Bowrampet, Hyderabad, Telangana, India
[6] Learning & Development Department, Mantra Softech India Pvt. Ltd, Ahmedabad, Gujarat, India
* Correspondence: jainrituraj@yahoo.com;

Citation:
Jain, R.; Bekele, K.S.; Palaniappan, D.; Parmar, K.; P B.R.; Trivedi M.A. Detection of COVID-19, pneumonia, and tuberculosis using convolutional neural networks and ensembleof deep learning architectures. *ASEAN J. Sci. Tech. Report.* **2025**, *28*(1), e253662. https://doi.org/10.55164/ajstr.v28i1.253662

Article history:
Received: May 22, 2024
Revised: October 16, 2024
Accepted: November 9, 2024
Available online: February 16, 2025

Publisher's Note:
This article has been published and distributed under the terms of Thaksin University.

Abstract: Testing, diagnosis, and treatment must be done quickly in the current scenario, where the COVID-19 pandemic continues to affect the world's health. Pneumonia and Tuberculosis (TB) are always very concerning chest diseases, and COVID-19 has also been added to this list. Chest X-rays (CXR) and CT scans are major sources for diagnosing respiratory disorders. As CT scans are a little bit costlier and take more time, as well as expose patients to mild radiation, the use of CXR is increasing for the diagnosis of chest diseases. This study uses CXR images to accurately identify diseases using the developed MobileNetV2, ResNet50, VGG19, and DenResCov-19 Convolutional Neural Network (CNN). The models were analyzed and tested using the publicly available 13805, 5840, and 4200 chest x-ray images for COVID-19, pneumonia, and TB cases. The in-house mobile app employs a variety of deep-learning models to identify diseases from chest X-rays. With 99.79% accuracy and 96.89% F1-score, ResNet50 is the best model architecture for COVID-19 classification. The ResNet50 pneumonia classification model was 99.17% accurate and had an F1-score of 94.52%. With 99.88% TB detection accuracy and 99.64% F1-score, MobileNetV2 and ResNet50 were equivalent. Comparing model efficacy on the dataset was fascinating.

Keywords: CNN, COVID-19, Pneumonia, Radiography, Tuberculosis

1. Introduction

The lungs play a vital role in the human physiological system as they undergo expansion and contraction processes to facilitate oxygen intake and carbon dioxide expulsion. Lung disorders encompass a range of respiratory ailments that impact respiration's physiological structures and functions, leading to conditions affecting the airways, lung tissues, and pulmonary circulation. Certain respiratory infections, such as the common cold and influenza, may result in minimal discomfort and annoyance. However, there are other respiratory infections, such as pneumonia, TB, and lung cancer, that pose a significant threat to life and lead to the development of severe acute respiratory

complications. The early detection of the illnesses above during the initial stages of infection can significantly enhance the likelihood of survival and mitigate human fatalities. Chest radiography and Computed Tomography (CT) imaging are commonly employed diagnostic procedures for identifying and assessing these conditions [1,2].

In recent decades, medical practitioners have encountered challenges in accurately diagnosing diseases, leading to needless interferences in healthcare and malpractice litigation for stakeholders. Many studies conducted through interdisciplinary collaboration between medical and engineering researchers have extensively investigated the effectiveness of computer-aided diagnosis within the medical domain. Some automated diagnosis systems utilized in medicine can also be classified as expert systems due to their aim of emulating the diagnostic reasoning of medical experts. Furthermore, it is worth noting that computer-aided detection systems utilized in medicine can effectively analyze intricate and substantial volumes of clinical data [3]. Computer-aided detection systems have the potential to assist doctors in gaining novel perspectives on data and utilizing acquired knowledge to enhance diagnostic precision. Because of this, the systems are considered intelligent because they use feedback methods to improve their efficiency over time.

The most recent advancements in analysis and classification tools rely on Machine Learning (ML) applications and DL techniques, demonstrating their effectiveness as computer-based tools. Recent advancements and investigations in ML and DL have demonstrated that automated tools have yielded remarkable outcomes surpassing those achieved by human identification in several application domains. Figure 1 illustrates the sequential stages of identifying features and subsequent categorization using image processing techniques on datasets, including CXR or CT images. ML and DL systems can effectively incorporate and analyze vast datasets to facilitate system learning and provide accurate predictions. The main goals of DL models are to discover and classify image properties within extensive datasets accurately. Most contemporary thriving industries, such as healthcare, have attained very impactful discoveries through DL-based systems [4]. DL may also be employed to develop systems capable of adequately predicting and diagnosing diseases based on visual data. Previous studies have shown evidence of the efficacy of this approach in the detection of TB [5-9], pneumonia [10-18], and COVID-19 [11, 15, 18-25] without the need for human interaction. The subsequent sections of the manuscript are organized in the following manner: The second half of the material delves into the principles and theories around convolutional neural networks. Section 3 analyzes and examines relevant scholarly contributions within the existing body of literature. Section 4 provides an overview of the approach employed in the proposed system, while Section 5 presents a concise summary of the findings obtained from the system.

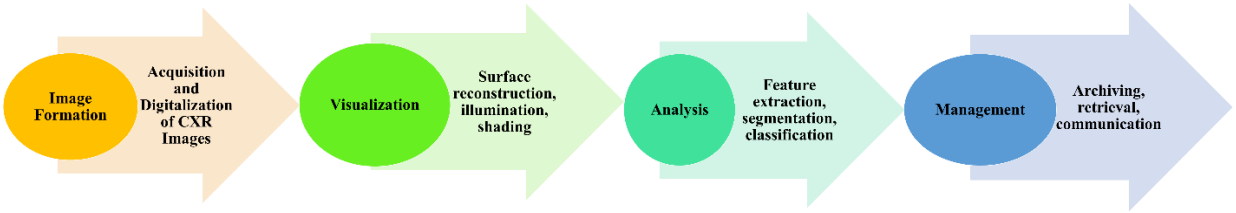

Figure 1. Representation of classification model based on image processing

2. Convolutional Neural Networks (CNNs) Architecture

CNNs are highly successful in recognizing and classifying features within image datasets. The architecture consists of three distinct layers, namely convolutional, pooling, and fully-connected layers. The convolutional approach employed by the convolutional layer facilitates the identification and extraction of the primary features inherent in the collection of images. Convolution kernels and learnable filters facilitate the extraction of internal image characteristics and deep vital data. To validate the output of the neurons, the dot product between the weight of the kernel and the local region will be utilized. Equation 1 illustrates the convolution process.

$$z = w_i^l * y^{(j)} \tag{1}$$

where * represents a cross product of weight and local regions of the kernel, W_i^l is the weights of the 1st layer ith filter kernel for CNN, and $y^{(j)}$ is the 1st layer's jth local region of CNN.

To use neural networks to solve complex problems, it is necessary to use a convolution operation, followed by the utilization of an activation function, such as sigmoid, Rectified Linear Units (ReLU), and so on. The function above generates the activation map, which encompasses the filter responses. ReLU outperforms classic activation functions such as sigmoid and tanh due to its ability to accelerate the training of neural networks by a factor of four, leading to reduced computational expenses. The ReLU function is defined by (2) [26], where *y* is the input.

$$g(y) = \begin{cases} 0 \ for \ y < 0 \\ y \ for \ y \geq 0 \end{cases} \tag{2}$$

Similarly, the incorporation of the last layer involves the utilization of the SoftMax activation function, which serves to enhance the efficacy of the neural network. The SoftMax function is given in (3) [26].

$$\sigma(c)_j = \frac{e^{z_i}}{\sum_{j=1}^{K} e^{z_j}} \tag{3}$$

where z_i is the raw output (logit) of class *I*, *K* is the total number of classes, and e is the base of the natural logarithm (approximately equal to 2.71828).

In addition to including convolution layers, CNNs have pooling layers responsible for processing the output generated by the convolution layers. The fundamental aim of the pooling layer is to decrease the dimensions of the feature map, resulting in compression while preserving relevant information. This will lead to decreased computation times and less overfitting. CNN attains a heightened degree of awareness through many iterations of convolution and pooling layers, ultimately leading to the integration of fully connected (FC) layers. The weights and biases implemented in these layers facilitate connectivity between neurons of different layers. The fully connected layer's final layer consists of as many output neurons as there are classes to be recognized. The categorization procedure makes use of this layer.

ResNet50 is one of the family of Residual Networks members, which overcame the problem of vanishing gradients in deep networks and was completed using skip connections. It became possible to train such a network efficiently, even with 50 layers. This design incorporates several residual blocks, whereby every block is built from convolutional layers followed by batch normalization and ReLU activation to ensure smooth propagation of the gradients. ResNet50 is typically utilized for applications where high accuracy is needed. It can take input images of size 224x224 pixels. VGG19 was one of the early influential CNN architectures with a deep and simple structure. It contains 16 stacked small 3x3 filter convolutional layers followed by three fully connected layers at the tail end. Although the network is deep, applying max pooling after stacks of convolutional layers is pretty straightforward. This architecture also accepts 224x224 pixel images and has become a benchmark model for various image classification tasks due to reliable performance.

MobileNetV2 is designed with efficiency in mind, especially in mobile and edge device settings where one does not have too much computational power. This architecture uses depthwise separable convolutions that split the operation of convolutions into two parts: depthwise and pointwise. They result in an extremely low number of parameters and computational cost. Further, MobileNetV2 uses linear bottlenecks and residual connections important for fast information flow. Its design is applied when simultaneous high accuracy and high-speed performance are desired without heavyweight hardware. Another crucial CNN architecture based on dense connections within the layers is DenseNet, particularly in its use as DenResCov-19 for detecting COVID-19. In DenseNet, every layer is given input from all layers that have been processed previously to boost feature propagation and reduce the number of parameters needed while enhancing gradient flow. Generally, DenseNet is composed of a series of dense blocks, the transitions of which are followed by a

reduction in the dimensionality of the feature maps. Because of its strong feature extraction capabilities, this architecture has proven useful in medical imaging tasks, such as detecting COVID-19 diseases.

There have been several attempts to determine whether or not DL models help predict COVID-19, pneumonia, and TB. Due to its ability to assist in the automatic identification of viruses in medical imaging modalities like CT scans and X-rays, DL has seen widespread use in the field of diagnostics. Patterns and characteristics linked to COVID-19, pneumonia, and TB have been successfully identified with the help of CNN. One proposed approach for successful DL-based COVID-19 screening is a voting-based technique pioneered by Silva and Luz. It has achieved higher accuracy than existing state-of-the-art approaches [19]. Using multi-modality data and clinical specialists' views is crucial for ensuring accurate and efficient diagnosis of COVID-19 since treating each CT imaging slice independently might lead to potentially misleading outcomes [19,20]. AI-based approaches have been commonly employed for COVID-19 screening, diagnosis, and prediction. However, there are issues with their ability to generalize due to the training and testing process using images from the same dataset [19,21]. DL methods, specifically CNN, Recurrent Neural Networks (RNN), and Long Short-Term Memory (LSTM), have been utilized to identify, diagnose, and classify COVID-19. These approaches have demonstrated encouraging outcomes, even with limited data availability [20,21]. In addition to DL methods, many other ML techniques, such as Support Vector Machines (SVM), logistic regression, random forests, and decision trees, have been effectively employed to identify and predict the severity of COVID-19 [21,22]. The methodologies above have been employed to simulate patient outcomes and forecast the degree of severity, likelihood of ICU admission, and fatality rates. These predictions are derived from an analysis of clinical factors, blood tests, and quantitative CT parameters [22].

In general, using artificial intelligence (AI) and ML in medical imaging has improved the accuracy of diagnosing COVID-19 by analyzing CXR and CT images. Furthermore, integrating several modalities in AI models can enhance the intelligence of medical systems in diagnosing and predicting COVID-19 [20]. However, it is worth noting that DL has exhibited impressive results in the context of COVID-19 applications. This is exemplified by the Truncated Inception Net, a CNN model based on DL techniques. The model above has achieved a remarkable accuracy of 99.96% in identifying COVID-19-positive cases, distinguishing them from patients with pneumonia and those in good condition [23]. Similarly, the AI system CAD4COVID-XRay identified CXR images explicitly as COVID-19 pneumonia with an AUC of 81%, making it effective in low-resource situations where diagnostic equipment is not accessible [23]. However, establishing trust in DL models' accuracy is crucial before investing resources in developing drugs to attack protein targets identified by the models [24]. The paper extensively examines existing literature concerning the present state and prospective advancements in utilizing DL techniques for detecting COVID-19 [23,25].

The identification of TB using automated means has garnered considerable interest in recent years, resulting in several scholarly articles that showcase cutting-edge DL methodologies. A thorough examination of the existing literature has been carried out to explore the use of DL methods in identifying TB. This review aims to support researchers in creating a Computer-Aided Diagnosis (CAD) system that can effectively diagnose TB by employing DL classifiers. The review emphasizes the need to assess the precision of CAD systems by employing distinct datasets for evaluation, apart from those used for training. Additionally, it underscores the need to acknowledge the constraints present in current studies regarding methodologies and stated accuracy to inform the development of CAD systems in subsequent research endeavors. This study primarily centers on using DL classifiers to diagnose TB through the analysis of CXR. Numerous DL approaches have been employed for TB screening, prediction, and diagnosis. It isn't easy to compare the approaches due to several aspects, such as the types of datasets used, the number of image samples, the assessment metrics employed, and the tuning of model parameters [27]. In the current era of new technologies, ML and DL techniques are prevalent in diagnosing TB using indicators from a dataset of chest radiographs, sputum smears, and biomarkers sources [28]. The progression of CAD adheres to a conventional structure comprising four distinct stages: pre-processing, segmentation, feature extraction, and classification. Pre-trained CNNs have been employed to train extensive datasets such as the RSNA, Pediatric pneumonia, and Indiana datasets. This utilization has enhanced accuracy in TB diagnosis utilizing modality-specific DL

models. The feature extraction process entails identifying discriminative characteristics utilized for further investigation [27]. Furthermore, prior methodologies for TB detection have utilized pre-trained CNN models. Additionally, TB diagnosis has been carried out using techniques such as handcrafting, ML, and DL, as mentioned in reference [28]. The study's primary objective was to examine the CAD system, utilizing one or more DL approaches as the classifier for TB detection [27].

In [29], the authors highlighted the significant capacity of DL to transform the diagnosis and treatment of respiratory illnesses. DL systems demonstrate a high skill level in accurately diagnosing different lung illnesses by analyzing complex patterns in large datasets. This advancement not only improves the process of making medical decisions but also has the potential to influence the treatment of respiratory diseases significantly. Moreover, using extreme learning machine approaches offers an additional approach to identifying respiratory disorders, particularly the urgent issue of COVID-19 [30]. By utilizing the efficient structure of Convolutional Neural Networks (CNNs), these algorithms are highly effective in extracting essential characteristics from medical images, enabling precise illness identification. The partnership between CNN architecture and extreme learning machines highlights a viable strategy for enhancing healthcare results, specifically in respiratory health[30]. Authors of [31] have significantly contributed to this subject by creating a Chest Infection Diagnostic Model. Using transfer learning and a multistage multiclass architecture, this model improves accuracy in diagnosing a wide range of chest diseases, including common colds and severe pneumonia. These developments give healthcare personnel more accurate diagnostic abilities, potentially improving patient care and outcomes.

Incorporating artificial intelligence (AI) and knowledge distillation techniques in CAD systems represents a notable advancement in diagnosing pneumonia, TB, and COVID-19 [32]. By condensing information from intricate AI models into more efficient systems, these CAD platforms demonstrate remarkable precision comparable to human specialists in analyzing chest radiographs. The combination of AI-driven innovation and medical imaging holds great promise for the future of precision medicine and the accuracy of diagnostics [32]. DL plays a crucial role in CT imaging for accurately categorizing respiratory illnesses such as pneumonia, TB, and COVID-19. By analyzing large CT datasets, DL algorithms may detect tiny patterns that suggest certain illnesses. This enables the early and accurate detection of diseases. This innovative method has great promise for enhancing medical diagnostics and patient outcomes in chest illnesses [33].

The emergence of Vision Transformers signifies state-of-the-art progress in identifying pneumonia using chest X-ray images. By harnessing sophisticated ML algorithms, Vision Transformers efficiently process images to detect distinctive indicators of pneumonia, facilitating prompt interventions and ultimately preserving lives. The integration of technology and healthcare highlights the profound capacity of artificial intelligence to revolutionize illness detection and patient treatment [34].

A deep transfer learning convolutional neural network approach was proposed by Sai et al. (35), which can distinguish between viral pneumonia, bacterial pneumonia, and COVID-19. The training dataset consisted of 5856 chest radiographs, which were used to train a pre-trained ResNet-50V2 model for 100 epochs. The training method resulted in an accuracy rate and test score of 94%. The attainment of a high level of precision was aided by increasing the number of epochs and incorporating a dropout layer following the dense layer. The CNN (Convolutional Neural Network) architecture is commonly employed for binary and multiclass classification tasks. The training dataset consisted of 3877 CT and X-ray images, with 1917 of them being of patients diagnosed with COVID-19. The performance of the binary classifier was evaluated, yielding an accuracy of 99.64%.

Additionally, the classifier demonstrated a recall rate of 99.58%, precision of 99.56%, F1 score of 99.59%, and a perfect receiver operating characteristic (ROC) score of 100%. A total of 6077 images were utilized for training the model. The number of individuals diagnosed with COVID-19 was 1917, whereas 1960 individuals were deemed healthy. Additionally, there were 2200 reported occurrences of pneumonia. The authors reported accuracy, sensitivity, precision, F1-score, and ROC values of 98.28%, 98.25%, 98.22%, 98.23%, and 99.87% correspondingly for the multiclass classification [36].

To speed up the COVID-19 diagnostic process, Oguz et al. [37] employed a dataset of 1345 CT scan images acquired from a research hospital. The images are subjected to various DL algorithms, such as ResNet-50, ResNet-101, AlexNet, and GoogleNet, as well as additional categorization techniques like SVM, Random Forest, Decision Trees, and others. During the pre-processing phase, the dimensions of the CT images were decreased by implementing maximum pooling. In addition, the Rectified Linear Unit (ReLU) activation function was included in each convolutional layer. The experimental findings indicated that ResNet-50 and SVM outperformed the other models, achieving an accuracy rate of 96.3% and an F1-score of 95.87%. Nevertheless, the effectiveness of this methodology is constrained by the amount of data used and may not demonstrate robust applicability to unfamiliar data. As the quantity of utilized classes increases, there is a corresponding drop in the model's accuracy. Hussain et al. [38] presented their findings, showcasing the development of a deep Convolutional Neural Network model named 'CoroDet,' consisting of 22 layers. The dataset utilized in this study comprised a total of 7390 images, with 2843 images representing COVID-19 patients, 3108 images representing normal cases, and 1439 images representing instances of pneumonia caused by both viral and bacterial infections. The deep Convolutional Neural Network model was utilized for three distinct class classifications: COVID-19, Pneumonia-Bacteria, and Normal. A four-class classification, including COVID-19, Pneumonia-Bacteria, Normal, and Pneumonia-Viral, was also performed. Notably, no preprocessing of the data was conducted before these classifications. The methodology devised by the researchers resulted in an accuracy rate of 99.1% for classifiers with two classes, 94.2% for classifiers with three classes, and 91.2% for classifiers with four classes. Nevertheless, these conclusions may be enhanced by the augmentation of data, equalizing class instances, and implementing data pre-processing techniques to mitigate noise.

3. Materials and Methods

This research aims to construct a DL framework that can accurately categorize COVID-19, Pneumonia, and TB into normal and pathological categories. The suggested system employs a DL convolutional neural network. Its main use is image categorization and analysis, where each network layer applies a distinct set of filters. The outcomes of each layer are obtained by the fusion of a range of 100 to 1000 filters. The results are ultimately transmitted to the subsequent neural network layer. Figure 2 illustrates the suggested methodology for the detection model, which aims to distinguish normal and infected cases for each illness. The training process utilizes the Keras and Tensorflow software libraries. The proposed model would incorporate many stages, including dataset acquisition, partitioning, preprocessing, training, and testing/evaluation.

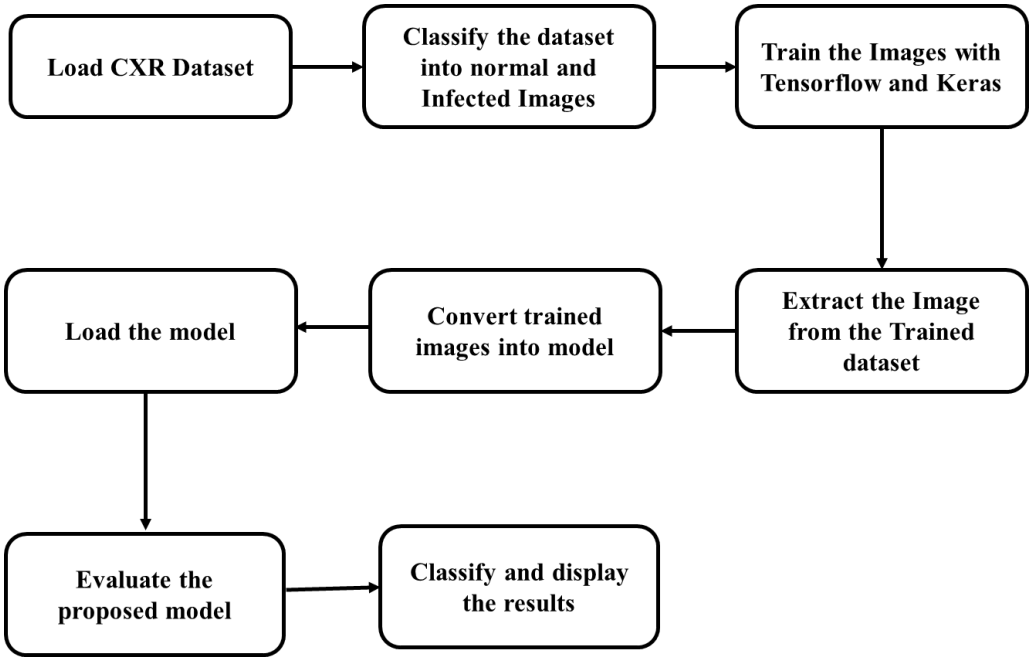

Figure 2. Proposed system's framework

Figure 3 shows the block diagram of the proposed system. The proposed model takes as input X-ray samples of images associated with each detected disease. The first convolutional layer receives image input, which is processed using a specified activation function. The pooling layer is introduced successively after the activation function layer. The utilization of a max pooling layer serves the purpose of diminishing the spatial dimensions of the representation. The suggested model includes a secondary convolutional layer that follows the same layer sequence as the first layer, including an activation layer, a pooling layer, and a max-pooling layer.

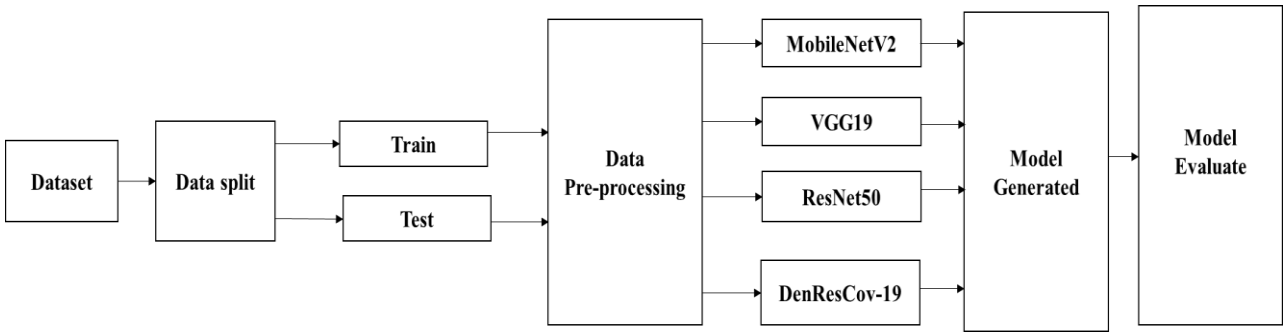

Figure 3. Block diagram of the proposed system

In the initial stage, the input images are subjected to a random partitioning method, whereby the data image is divided into 80% for training purposes and 20% for validation. Pre-processing techniques such as normalization and scaling are also applied to the images using relevant functions. Then, in the second and third stages, DL algorithms are deployed. The second step involves the process of feature extraction, which is achieved by employing ResNet50, VGG19, MobilenetV2, DenResCov-19, and CNN algorithms. Employing a fully linked network is utilized at the image categorization stage.

The architecture of the CNN, as outlined in section 2 and depicted in figure 4, comprises an input layer, an output layer, and hidden layers that are formed of convolutional layers with Rectified Linear Units (ReLU), pooling layers, and fully connected layers. The input datasets for this network consist of X-ray images representing both normal and sick occurrences for each illness, along with three RGB channels. The dimensions of the chosen input data set are 224 x 224. The provided dataset is inputted into the first layer, known as the convolutional layer, which utilizes the Rectified Linear Unit (ReLU) activation function. The initial layer employs a kernel with the size of 224 x 224 and produces 32 output channels to diminish the feature map. Additionally, it generates 32 output channels to further lower the feature map to a size of 112. The maximum values for each window will be documented when filtered using the stride. The procedure above will be executed for every individual dataset of filtered images. The third layer of the network consists of a convolutional layer with a kernel size of 112 x 112, followed by a pooling layer with a kernel size of 7 x 7, which precedes the fully connected layer. Furthermore, the network incorporates a flattened layer that is fully linked. The SoftMax function incorporates a fully linked layer into the model architecture. The ultimate layer will be employed to make predictions regarding the classification of an image, namely whether it is normal or contaminated with a disease.

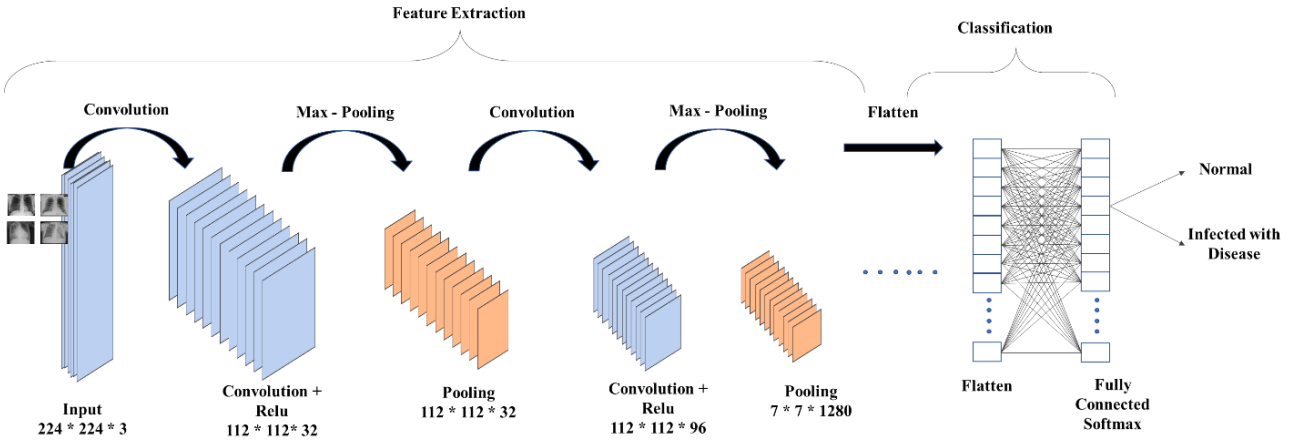

Figure 4. CNN model architecture used for the proposed system

3.1 Dataset

In addition to healthy examples, X-ray images of COVID-19, pneumonia, and TB were accessible and collected from dependable sources [38-40]. Figure 5 presents X-ray image samples utilized in this work, showcasing (A) a normal case, (B) a case of COVID-19, (C) a case of pneumonia, and (D) a case of TB. The COVID-19 dataset comprises 13,805 images, encompassing both normal and diseased cases. These images are further separated into 11,044 for training and 2,761 for testing purposes. The dataset consists of a total of 5840 images, encompassing both normal and infected instances of pneumonia. These images are further separated into 4672 images for training and 1168 images for testing purposes. The dataset used in this study consists of a total of 4200 images, encompassing both normal and infected instances of pneumonia. These images have been separated into two subsets: 3360 images for training purposes and 840 images for testing purposes. Table 1 presents the specific information of the dataset stated before.

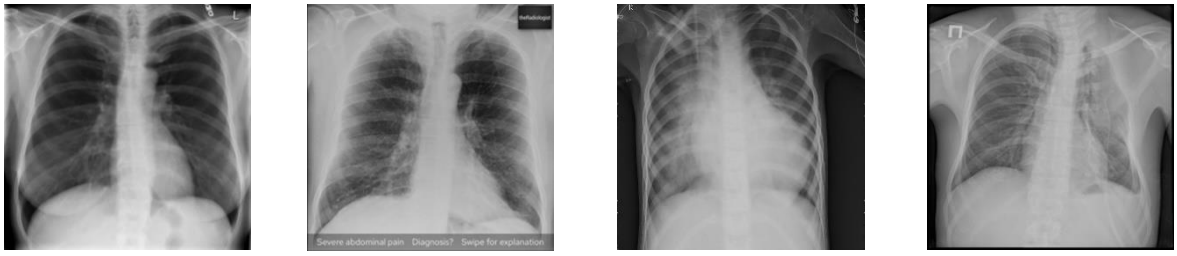

(a) (b) (c) (d)

Figure 5. X-ray image samples (a) normal (b) COVID-19 (c) pneumonia (d) tuberculosis

3.2 Preprocessing and Data Augmentation

The datasets comprise X-ray images with varying resolutions. In contrast, the CNN models require the image dataset to adhere to specific size requirements. Consequently, the X-ray images within the dataset were uniformly scaled to dimensions of 224 * 224. Decreasing the dimensions of the input image has the effect of expediting the image processing procedure, hence hastening the model's performance for the specific associated job. The primary concern associated with image datasets is overfitting. Data augmentation is a widely employed strategy in ML, wherein small alterations are introduced to an image during each training epoch. This approach is favored due to its ability to substantially augment the volume of training data and effectively mitigate the issue of overfitting. Several augmentation techniques were employed in this study, encompassing image rotation, range shearing, range zooming, and horizontal flips.

Using a random splitting method, the dataset was divided into two subsets, namely the validation subset and the training subset. The validation subset accounted for 20% of the data, while the training subset

accounted for 80%. This division was implemented to ensure that the variability included in the X-ray images adhered to the required parameters for training the proposed model. The CNN model's ability to leverage additional data beyond the original dataset is essential for attaining high levels of accuracy.

Table 1. Details of Dataset of COVID-19, pneumonia, and tuberculosis used for this research study

Dataset of Diseases	Types of Images	Training Images	Testing Images	Total Images
COVID 19 [38]	Normal	8152	2038	10,190
	COVID 19 Infected	2892	723	3,615
	Total	11044	2761	13805
Pneumonia [39]	Normal	1260	315	1,575
	Pneumonia Infected	3412	853	4,265
	Total	4672	1168	5840
Tuberculosis [40]	Normal	2800	700	3500
	Tuberculosis Infected	560	140	700
	Total	3360	840	4200

3.3 System Realization

The present study employs an Android application developed internally utilizing the Arduino integrated development environment (IDE). The DL model was deployed on the web using Tensorflow.js, while the same model was deployed on an Android-based application using the Tensorflow-Lite API. The system underwent testing using datasets to verify its ability to recognize both normal and disease-infected instances and assess the performance of the developed model software program, which operated as anticipated. Figure 6 (a), (b), and (c) illustrate the Android applications that were built for this study.

4. Results and Discussion

The present study aimed to evaluate the performance of four different CNN models, MobileNetv2, VGG19, ResNet50, and DenResCov-19, in identifying COVID-19, Pneumonia, and TB. The models underwent training, during which their precision and losses were evaluated. Subsequently, the test efficacy was measured and compared to findings from other studies. In all experimental trials, the parameter values employed for the number of epochs, batch size, and dropout were 50, 32, and 0.5, respectively. The dataset was partitioned into 80% training and 20% testing sets. The experimental hardware consisted of an Intel i7-10750H processor. The GPU is Nvidia GTX 1660Ti, and RAM is 16GB.

The dataset images were classified into two groups, normal and afflicted with illness, using our suggested system that underwent training for 20 epochs. The accuracy, loss curves, and confusion matrix of the COVID-19 detection model using MobileNetv2, VGG19, ResNet50, and DenResCov-19 are depicted in Figures 7(a), (b), (c), and (d) accordingly. These figures illustrate the models' performance throughout the training and validation phases, spanning a total of 20 epochs. Likewise, the outcomes for Pneumonia and TB are demonstrated by 8(a), (b), (c), (d) and 9(a), (b), (c), (d).

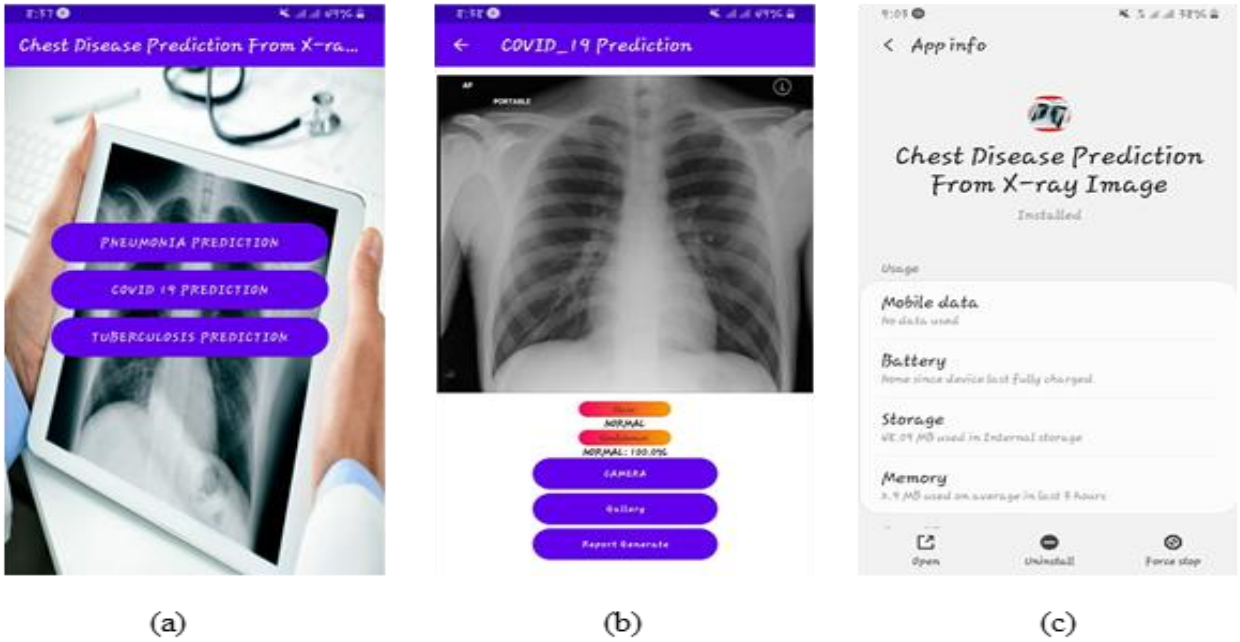

Figure 6. Android App developed for the realization of the proposed system

Table 2 presents comprehensive data about the accuracy and loss metrics for training and validation phases over 20 epochs for each model of COVID-19, Pneumonia, and TB.

Table 2. Accuracy % and loss in training and validation over 50 epochs of detection model using MobileNetV2, VGG19, ResNet50, DenResCov-19

Disease Name	Model Name	Accuracy %		Loss	
		with the training dataset	with the validation set	with the training dataset	with the validation set
COVID-19	MobileNetV2	99.36	97.39	0.0219	0.0729
	VGG19	97.96	94.97	0.0619	0.0128
	Resnet50	99.79	98.37	0.0094	0.0556
	DenResCov-19	99.24	97.72	0.029	0.068
Pneumonia	MobileNetV2	99.12	96.92	0.0309	0.1004
	VGG 19	98.39	96.58	0.0512	0.1023
	Resnet50	99.17	97.09	0.0271	0.0852
	DenResCov-19	98.42	96.23	0.0473	0.0934
Tuberculosis	MobileNetV2	99.89	99.4	0.0011	0.0154
	VGG 19	99.82	99.4	0.0075	0.0207
	Resnet50	99.88	99.4	0.0012	0.0181
	DenResCov-19	99.77	99.29	0.0023	0.0195

The loss curves in Figures 7, 8, and 9 demonstrate a minimal discrepancy between the training and validation loss curves, suggesting that the models have achieved satisfactory convergence. Furthermore, no indications of overfitting were seen throughout the training and validation processes. The confusion matrix is employed to represent the system's performance metrics. Additional assessment metrics can be developed using the available data to emphasize the system's performance being discussed. The confusion matrix yields a True Positive outcome when the system accurately classifies an infected case as the correct disease. A False Positive outcome occurs when the system incorrectly identifies a normal case as one of the disease cases. True

Negative is achieved when the system correctly classifies a normal case as normal, indicating the absence of disease. Lastly, a False Negative outcome arises when the system misclassifies an infected case as normal.

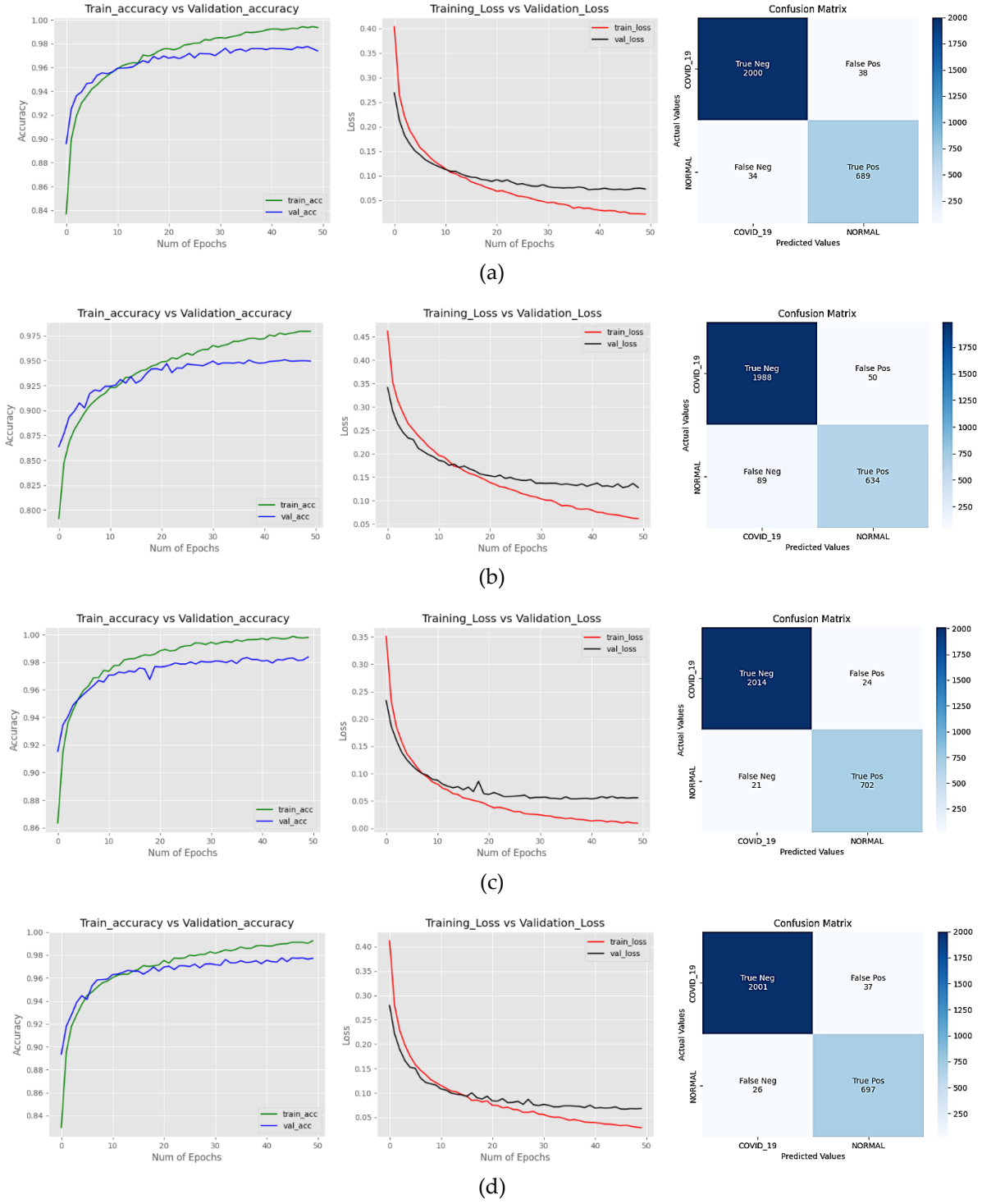

Figure 7. Accuracy curve, loss curves, confusion matrix of COVID-19 detection model using (a)MobileNetv2 (b)VGG19 (c)ResNet50 (d)DenResCov-19

An evaluation was undertaken to assess the performance of the classification model constructed in this study. This evaluation involved the consideration of several derived parameters: True Positive Rate (TPR), True Negative Rate (TNR), False Negative Rate (FNR), and False Positive Rate (FPR) as specified in (4-7) [41].

Additionally, performance metrics such as precision, accuracy, and F1 score, reported as in (8-10) [42], were also considered. The additional metrics, recall and specificity, are equivalent to the TPR described in (4) and the TNR outlined in (6).

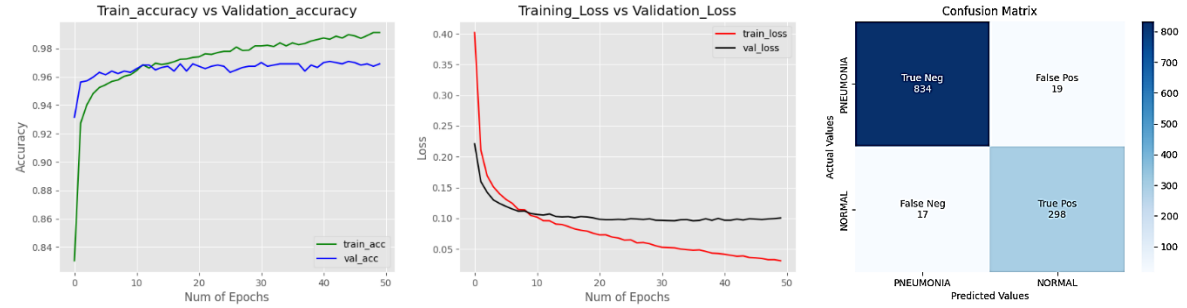

(a)

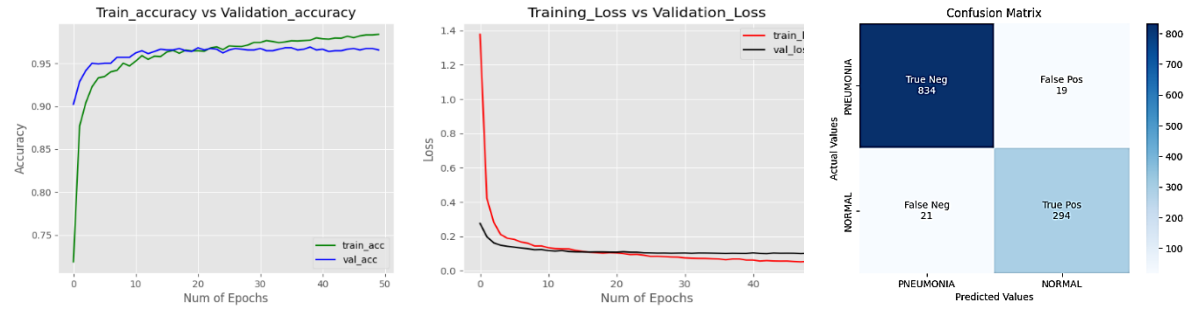

(b)

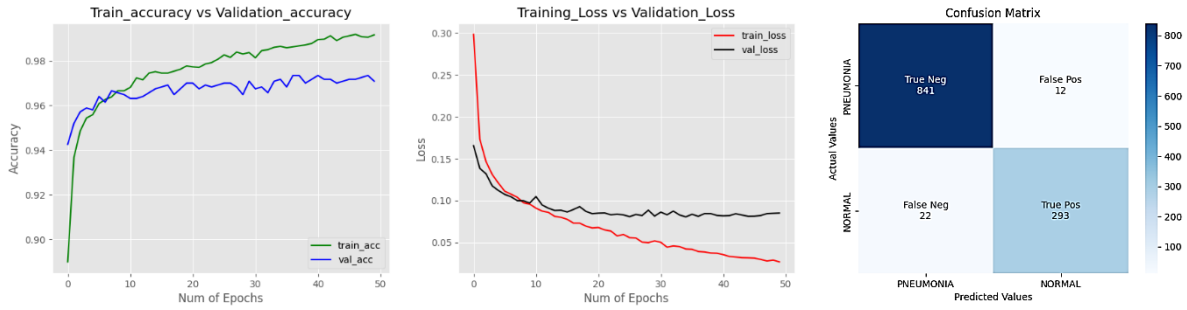

(c)

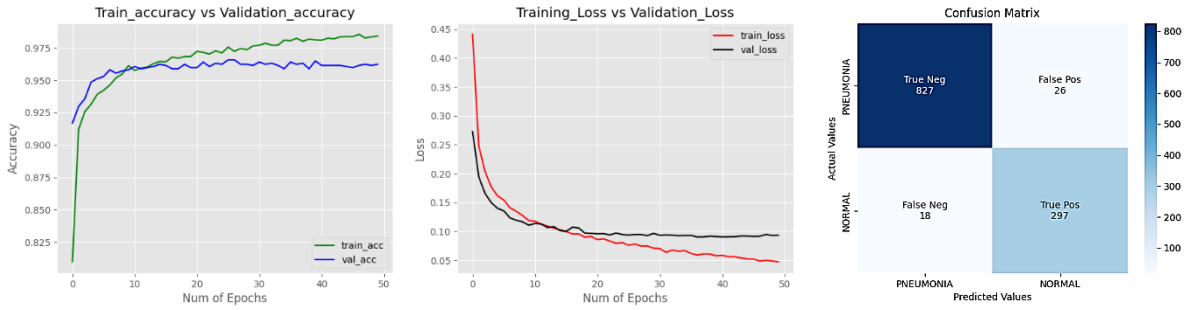

(d)

Figure 8. Accuracy curve, loss curves, confusion matrix of Pneumonia detection model using (a)MobileNetv2 (b)VGG19 (c)ResNet50 (d)DenResCov-19

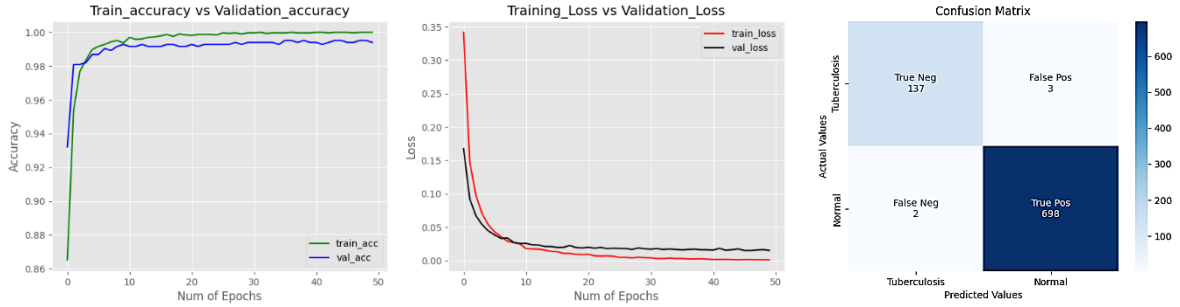

(a)

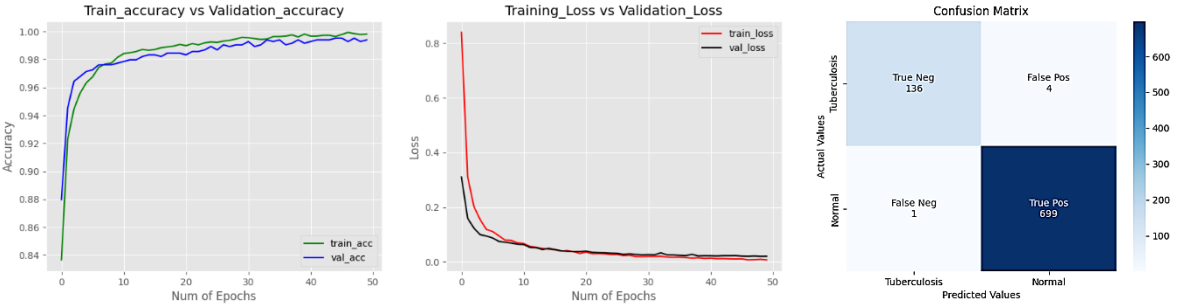

(b)

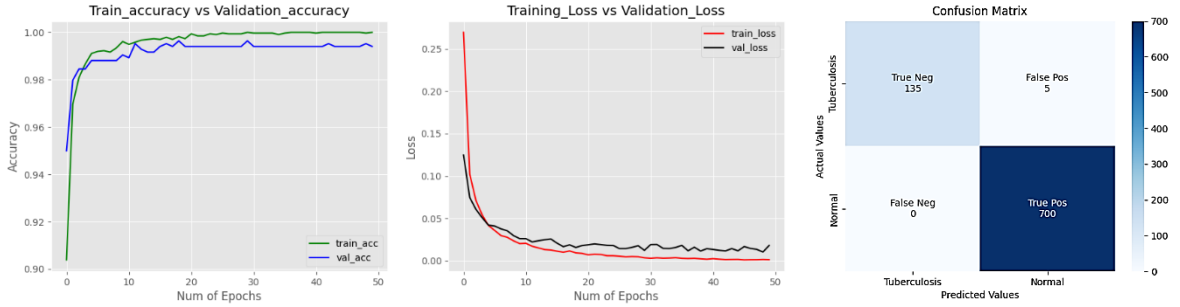

(c)

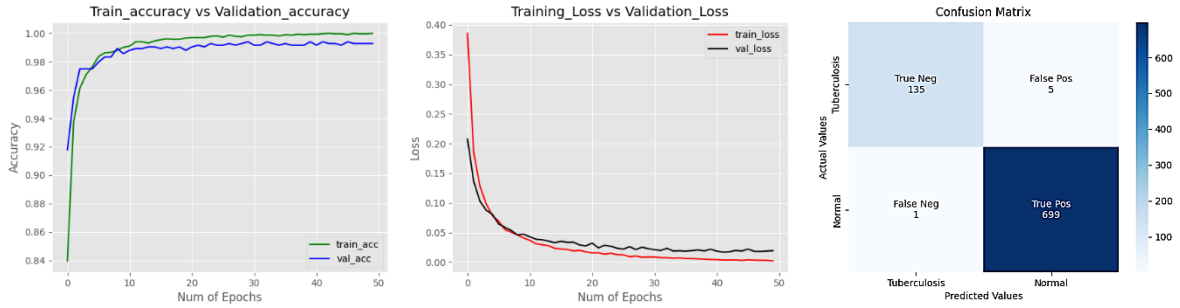

(d)

Figure 9. Accuracy curve, loss curves, confusion matrix of TB detection model using (a) MobileNetv2 (b) VGG19 (c) ResNet50 (d) DenResCov-19

$$TPR = \frac{Tpos}{Tpos + Fneg} \tag{4}$$

$$FNR = \frac{Fneg}{Tpos + Fneg} \tag{5}$$

$$TNR = \frac{Tneg}{Tneg + Fpos} \tag{6}$$

$$FPR = \frac{Fpos}{Tneg + Fpos} \tag{7}$$

$$\Pr ecision = \frac{Tpos}{Tpos + Fpos} \tag{8}$$

$$Accuracy = \frac{Tpos + Tneg}{Tpos + Tneg + Fpos + Fneg} \tag{9}$$

$$F1\ Score = \frac{2 * \Pr ecision * \mathrm{Re} call}{\Pr ecision + \mathrm{Re} call} \tag{10}$$

The assessment of precision functions as a method to measure the efficacy and feasibility of the proposed system. The precision metric is utilized to determine the true proportion of positive predictions. The recall measure, or the sensitivity measure, evaluates the proportion of correct predictions generated by the suggested model. The F1-score is commonly defined in academic literature as the inverse mean of the recall and accuracy metrics, which are widely employed for assessing the performance of a model. The equations above can provide a deeper understanding of the suggested system. The classification report of the suggested system is presented in Table 3.

According to the data shown in Table 3, it is evident that the ResNet50 model architecture outperforms the other models utilized in terms of performance. The ResNet50 model achieves an accuracy of 99.79% and an F1 score of 96.89% for COVID-19, while for pneumonia classification, it attains an accuracy of 99.17% and an F1 score of 94.52%. The performance of TB diagnosis using the MobileNetV2 and ResNet50 models exhibited nearly identical levels of accuracy, achieving a rate of 99.88%. The F1 score, which measures the balance between precision and recall, also reached 99.64%. One notable discovery in our research is the comparison of the efficacy of different models using the provided dataset.

Table 3. Performance evaluation of different measures for the proposed system

Disease Name	Model Name	Measures							
		TPR	FNR	TNR	FPR	Precision	Recall the same as TPR	Specificity same as TNR	F1-Score
COVID-19	MobileNetV2	0.9530	0.0470	0.9814	0.0186	0.9477	0.9530	0.9814	0.9503
	VGG19	0.8769	0.1231	0.9755	0.0245	0.9269	0.8769	0.9755	0.9012
	Resnet50	0.9710	0.0290	0.9882	0.0118	0.9669	0.9710	0.9882	0.9689
	DenResCov-19	0.9640	0.0360	0.9818	0.0182	0.9496	0.9640	0.9818	0.9568
Pneumonia	MobileNetV2	0.9460	0.0540	0.9777	0.0223	0.9401	0.9460	0.9777	0.9430
	VGG 19	0.9333	0.0667	0.9777	0.0223	0.9393	0.9333	0.9777	0.9363
	Resnet50	0.9302	0.0698	0.9859	0.0141	0.9607	0.9302	0.9859	0.9452
	DenResCov-19	0.9429	0.0571	0.9695	0.0305	0.9195	0.9429	0.9695	0.9310
Tuberculosis	MobileNetV2	0.9971	0.0029	0.9786	0.0214	0.9957	0.9971	0.9786	0.9964
	VGG 19	0.9986	0.0014	0.9714	0.0286	0.9943	0.9986	0.9714	0.9964
	Resnet50	1.0000	0.0000	0.9643	0.0357	0.9929	1.0000	0.9643	0.9964
	DenResCov-19	0.9986	0.0014	0.9643	0.0357	0.9929	0.9986	0.9643	0.9957

5. Discussion on Clinical Applicability

The proposed models, particularly ResNet50 and MobileNetV2, are now ready for application in clinical workflows to aid radiologists in determining these diseases quickly and efficiently: COVID-19, pneumonia, and tuberculosis. They have high accuracies at 99.79% for COVID-19 and 99.88% for tuberculosis, and these models might become a trustworthy tool for early detection, thus allowing for earlier management of patients and their treatments. With incredibly high accuracy rates obtained by the proposed models, they can be valuable tools supporting a radiologist's decision to make faster and more accurate diagnoses. This could become valuable where expertise by radiologists is fewer and farther between. The models used in this study- the MobileNetV2 especially- are highly computationally efficient and may be deployed even within resource-constrained environments. Where medical and CT scan professionals or units are difficult to access, the system may be a cost-effective and practical solution for disease detection and diagnosis by using only X-ray machines in a less densely populated or deprived area. The interface of proposed models into a mobile app will afford many telemedicine opportunities in which service providers can assess the X-rays taken by patients remotely. This could be particularly useful in the COVID-19 pandemic, where telemedicine diagnosis reduces contact exposure to healthcare workers and patients. Although these models demonstrate high performance on the datasets used here, the clinical environment may present a challenge, including noisiness, poor quality, or incompleteness of the X-ray images. Testing and validating the system in the clinical environment will be necessary to ascertain that the system can handle the variability associated with such situations.

6. Conclusions

Besides the ongoing COVID-19 pandemic, timely detection of diseases such as pneumonia and TB positively impacts patient mortality rates. To enhance the quality of healthcare services while minimizing expenses and reaction time, creating a mobile application that incorporates Convolutional Neural Networks and an Ensemble of DL Architectures is imperative. This application would be utilized inside energy-efficient medical devices to facilitate the automated identification of illnesses. An in-house mobile application of convolutional neural networks was developed using four different DL architecture models (MobileNetV2, ResNet50, VGG19, and DenResCov-19). These models were trained on COVID-19, pneumonia, and TB images from an open-access dataset. The models were utilized to classify the CXR image and discern the presence of COVID-19, pneumonia, TB, and healthy individuals. When evaluating several models for the detection of COVID-19, it was shown that the ResNet50 model architecture had superior performance, achieving an accuracy of 99.79%, an F1 score of 96.89%, and a precision of 96.69%. The ResNet50 model architecture demonstrates superior performance compared to previous models utilized in the detection of pneumonia, achieving an accuracy of 99.17%, an F1 score of 94.52%, and a precision of 96.07%. The performance of TB detection using the MobileNetV2 and ResNet50 models exhibited similar results, achieving an accuracy of 99.88% and 99.64% F1 score. Additionally, the precision rates for the MobileNetV2 and ResNet50 models were 99.57% and 99.29%, respectively. One of the noteworthy outcomes of our study is the comparison of the effectiveness of several models on the provided dataset. The entire data confirmed the proposed technique's efficacy and efficiency. In the foreseeable future, there will be a comprehensive collection of CT scan data, including data on diverse lung illnesses, to train the model and enhance the healthcare industry. All data sets were subsamples of specific sources, such as publicly available repositories like Kaggle, which would introduce geographic and institutional biases, potentially limiting the broader generalisability of the models to diverse populations or healthcare settings. For instance, the data can reflect particular demographic groups or medical institutions and thus may not represent more general populations in other parts of the world. Furthermore, validation in real-world clinical settings remains necessary since the proposed models were stringently tested on these datasets. Models might face noisy, low-quality, or ambiguous X-ray images in practical applications not found in this study's clean and preprocessing datasets. Testing in actual clinical environments would thus better give insight into the robustness and applicability of models to real-world challenges and variability in image quality.

Author Contributions: Conceptualization, methodology, testing, and writing—original draft preparation, R.J., S.B., D.P., K.P., R.P., and A.T.

Funding: This research received no external funding

Conflicts of Interest: The authors declare no conflict of interest.

References

[1] Shen, D.; Wu, G.; Suk, H.-I. Deep Learning in Medical Image Analysis. *Annual Review of Biomedical Engineering* **2017**, *19*(1), 221–248. https://doi.org/10.1146/annurev-bioeng-071516-044442

[2] Yanase, J.; Triantaphyllou, E. A systematic survey of computer-aided diagnosis in medicine: Past and present developments. *Expert Systems With Applications* **2019**, *138*, 112821. https://doi.org/10.1016/j.eswa.2019.112821

[3] Khan, M. A.; Quasim, M. T.; Alghamdi, N. S.; Khan, M. Y. A Secure Framework for Authentication and Encryption Using Improved ECC for IoT-Based Medical Sensor Data. *IEEE Access* **2020**, *8*, 52018–52027. https://doi.org/10.1109/access.2020.2980739

[4] Sathitratanacheewin, S.; Sunanta, P.; Pongpirul, K. Deep learning for automated classification of tuberculosis-related chest X-Ray: dataset distribution shift limits diagnostic performance generalizability. *Heliyon* **2020**, *6*(8), e04614. https://doi.org/10.1016/j.heliyon.2020.e04614

[5] Gao, X. W.; James-Reynolds, C.; Currie, E. Analysis of tuberculosis severity levels from CT pulmonary images based on enhanced residual deep learning architecture. *Neurocomputing* **2019**, *392*, 233–244. https://doi.org/10.1016/j.neucom.2018.12.086

[6] Hooda, R.; Mittal, A.; Sofat, S. Automated TB classification using ensemble of deep architectures. *Multimedia Tools and Applications* **2019**, *78*(22), 31515–31532. https://doi.org/10.1007/s11042-019-07984-5

[7] Chandra, T. B.; Verma, K.; Singh, B. K.; Jain, D.; Netam, S. S. Automatic detection of tuberculosis related abnormalities in Chest X-ray images using hierarchical feature extraction scheme. *Expert Systems With Applications* **2020**, *158*, 113514. https://doi.org/10.1016/j.eswa.2020.113514

[8] Lopes, U. K.; Valiati, J. F. Pre-trained convolutional neural networks as feature extractors for tuberculosis detection. *Computers in Biology and Medicine* **2017**, *89*, 135–143. https://doi.org/10.1016/j.compbiomed.2017.08.001

[9] Kumar, J. S.; Balamurugan, S. A. A.; Sasikala, S. Analysis of Deep Learning Techniques for Tuberculosis Disease. *SN Computer Science* **2021**, *2*(4). https://doi.org/10.1007/s42979-021-00680-y

[10] Rahimzadeh, M.; Attar, A. A modified deep convolutional neural network for detecting COVID-19 and pneumonia from chest X-ray images based on the concatenation of Xception and ResNet50V2. *Informatics in Medicine Unlocked* **2020**, *19*, 100360. https://doi.org/10.1016/j.imu.2020.100360

[11] Luján-García, J. E.; Yáñez-Márquez, C.; Villuendas-Rey, Y.; Camacho-Nieto, O. A Transfer Learning Method for Pneumonia Classification and Visualization. *Applied Sciences* **2020**, *10*(8), 2908. https://doi.org/10.3390/app10082908

[12] Stephen, O.; Sain, M.; Maduh, U. J.; Jeong, D.-U. An Efficient Deep Learning Approach to Pneumonia Classification in Healthcare. *Journal of Healthcare Engineering* **2019**, 2019, 1–7. https://doi.org/10.1155/2019/4180949

[13] Lascu, M.-R. Deep Learning in Classification of Covid-19 Coronavirus, Pneumonia and Healthy Lungs on CXR and CT Images. *Journal of Medical and Biological Engineering* **2021**, *41*(4), 514–522. https://doi.org/10.1007/s40846-021-00630-2

[14] Sirazitdinov, I.; Kholiavchenko, M.; Mustafaev, T.; Yixuan, Y.; Kuleev, R.; Ibragimov, B. Deep neural network ensemble for pneumonia localization from a large-scale chest x-ray database. *Computers & Electrical Engineering* **2019**, *78*, 388–399. https://doi.org/10.1016/j.compeleceng.2019.08.004

[15] Asnaoui, K. E. Design ensemble deep learning model for pneumonia disease classification. *International Journal of Multimedia Information Retrieval* **2021**, *10*(1), 55–68. https://doi.org/10.1007/s13735-021-00204-7

[16] Sirazitdinov, I.; Kholiavchenko, M.; Mustafaev, T.; Yixuan, Y.; Kuleev, R.; Ibragimov, B. Deep neural network ensemble for pneumonia localization from a large-scale chest x-ray database. *Computers & Electrical Engineering* **2019**, *78*, 388–399. https://doi.org/10.1016/j.compeleceng.2019.08.004

[17] Goyal, S.; Singh, R. Detection and classification of lung diseases for pneumonia and Covid-19 using machine and deep learning techniques. *Journal of Ambient Intelligence and Humanized Computing* **2021**, *14*(4), 3239–3259. https://doi.org/10.1007/s12652-021-03464-7

[18] Rahmani, A. M.; Azhir, E.; Naserbakht, M.; Mohammadi, M.; Aldalwie, A. H. M.; Majeed, M. K.; Karim, S. H. T.; Hosseinzadeh, M. Automatic COVID-19 detection mechanisms and approaches from medical images: a systematic review. *Multimedia Tools and Applications* **2022**, *81*(20), 28779–28798. https://doi.org/10.1007/s11042-022-12952-7

[19] Soomro, T. A.; Zheng, L.; Afifi, A. J.; Ali, A.; Yin, M.; Gao, J. Artificial intelligence (AI) for medical imaging to combat coronavirus disease (COVID-19): a detailed review with direction for future research. *Artificial Intelligence Review* **2021**, *55*(2), 1409–1439. https://doi.org/10.1007/s10462-021-09985-z

[20] Heidari, A.; Navimipour, N. J.; Unal, M.; Toumaj, S. The COVID-19 epidemic analysis and diagnosis using deep learning: A systematic literature review and future directions. *Computers in Biology and Medicine* **2021**, *141*, 105141. https://doi.org/10.1016/j.compbiomed.2021.105141

[21] Gomes, R.; Kamrowski, C.; Langlois, J.; Rozario, P.; Dircks, I.; Grottodden, K.; Martinez, M.; Tee, W. Z.; Sargeant, K.; LaFleur, C.; Haley, M. A Comprehensive Review of Machine Learning Used to Combat COVID-19. *Diagnostics* **2022**, *12*(8), 1853. https://doi.org/10.3390/diagnostics12081853

[22] Alafif, T.; Tehame, A. M.; Bajaba, S.; Barnawi, A.; Zia, S. Machine and Deep Learning towards COVID-19 Diagnosis and Treatment: Survey, Challenges, and Future Directions. *International Journal of Environmental Research and Public Health* **2021**, *18*(3), 1117. https://doi.org/10.3390/ijerph18031117

[23] Shorten, C.; Khoshgoftaar, T. M.; Furht, B. Deep Learning applications for COVID-19. *Journal of Big Data* **2021**, *8*(1). https://doi.org/10.1186/s40537-020-00392-9

[24] Rehman, A.; Iqbal, M. A.; Xing, H.; Ahmed, I. COVID-19 Detection Empowered with Machine Learning and Deep Learning Techniques: A Systematic Review. *Applied Sciences* **2021**, *11*(8), 3414. https://doi.org/10.3390/app11083414

[25] Bekele, S. K.; Gutema, M. G.; Tujuba, E. D.; Jain, R.; Bekuma, Y. IoT-Deep Learning Based Face Mask Detection System for Entrance and Exit Door. *International Journal of Electrical and Electronics Research* **2022**, *10*(3), 751–759. https://doi.org/10.37391/ijeer.100356

[26] Munadi, K.; Muchtar, K.; Maulina, N.; Pradhan, B. Image Enhancement for Tuberculosis Detection Using Deep Learning. *IEEE Access* **2020**, *8*, 217897–217907. https://doi.org/10.1109/access.2020.3041867

[27] Balakrishnan, V.; Kherabi, Y.; Ramanathan, G.; Paul, S. A.; Tiong, C. K. Machine learning approaches in diagnosing tuberculosis through biomarkers - A systematic review. *Progress in Biophysics and Molecular Biology* **2023**, *179*, 16–25. https://doi.org/10.1016/j.pbiomolbio.2023.03.001

[28] Jaiswal, A. K.; Tiwari, P.; Kumar, S.; Gupta, D.; Khanna, A.; Rodrigues, J. J. P. C. Identifying pneumonia in chest X-rays: A deep learning approach. Measurement **2019**, *145*, 511–518. https://doi.org/10.1016/j.measurement.2019.05.076

[29] Ahmed, M. S.; Rahman, A.; AlGhamdi, F.; AlDakheel, S.; Hakami, H.; AlJumah, A.; AlIbrahim, Z.; Youldash, M.; Khan, M. A. A.; Ahmed, M. I. B. Joint Diagnosis of Pneumonia, COVID-19, and Tuberculosis from Chest X-ray Images: A Deep Learning Approach. *Diagnostics* **2023**, *13*(15), 2562. https://doi.org/10.3390/diagnostics13152562

[30] Nahiduzzaman, Md.; Goni, M. O. F.; Islam, Md. R.; Sayeed, A.; Anower, Md. S.; Ahsan, M.; Haider, J.; Kowalski, M. Detection of various lung diseases including COVID-19 using extreme learning machine algorithm based on the features extracted from a lightweight CNN architecture. *Journal of Applied Biomedicine* **2023**, *43* (3), 528–550. https://doi.org/10.1016/j.bbe.2023.06.003

[31] Ali, M. U.; Kallu, K. D.; Masood, H.; Tahir, U.; Gopi, C. V. V. M.; Zafar, A.; Lee, S. W. A CNN-Based Chest Infection Diagnostic Model: A Multistage Multiclass Isolated and Developed Transfer Learning Framework. *International Journal of Intelligent Systems* **2023**, 2023, 1–12. https://doi.org/10.1155/2023/6850772

[32] Kabir, M. M.; Mridha, M. F.; Rahman, A.; Hamid, Md. A.; Monowar, M. M. Detection of COVID-19, pneumonia, and tuberculosis from radiographs using AI-driven knowledge distillation. *Heliyon* **2024**, *10*(5), e26801. https://doi.org/10.1016/j.heliyon.2024.e26801

[33] Kaewlek, T.; Tanyong, K.; Chakkaeo, J.; Kladpree, S.; Chusin, T.; Yabsantia, S.; Udee, N. Classification of Pneumonia, Tuberculosis, and COVID-19 on Computed Tomography Images using Deep Learning. *Trends in Sciences* **2023**, *20*(11), 6974. https://doi.org/10.48048/tis.2023.6974

[34] Singh, S.; Kumar, M.; Kumar, A.; Verma, B. K.; Abhishek, K.; Selvarajan, S. Efficient pneumonia detection using Vision Transformers on chest X-rays. *Scientific Reports* **2024**, *14*(1). https://doi.org/10.1038/s41598-024-52703-2

[35] Monowar, K. F.; Hasan, Md. A. M.; Shin, J. Lung Opacity Classification With Convolutional Neural Networks Using Chest X-rays; 11th International Conference on Electrical and Computer Engineering (ICECE), *IEEE*, **2020**. https://doi.org/10.1109/icece51571.2020.9393135

[36] Oğuz, Ç.; Yağanoğlu, M. Detection of COVID-19 using deep learning techniques and classification methods. *Information Processing & Management* **2022**, *59*(5), 103025. https://doi.org/10.1016/j.ipm.2022.103025

[37] Hussain, E.; Hasan, M.; Rahman, M. A.; Lee, I.; Tamanna, T.; Parvez, M. Z. CoroDet: A deep learning based classification for COVID-19 detection using chest X-ray images. *Chaos Solitons & Fractals* **2020**, *142*, 110495. https://doi.org/10.1016/j.chaos.2020.110495

[38] COVID-19 Radiography Database. Kaggle. https://www.kaggle.com/datasets/tawsifurrahman/covid19-radiography-database (accessed 2024-02-19).

[39] Chest X-Ray Images (Pneumonia). Kaggle. https://www.kaggle.com/datasets/paultimothymooney/chest-xray-pneumonia/code?resource=download (accessed 2024-02-17).

[40] Tuberculosis (TB) Chest X-ray Database. Kaggle. https://www.kaggle.com/datasets/tawsifurrahman/tuberculosis-tb-chest-xray-dataset (accessed 2024-02-10)

[41] Rahman, M. M.; Manik, Md. M. H.; Islam, Md. M.; Mahmud, S.; Kim, J.-H. An Automated System to Limit COVID-19 Using Facial Mask Detection in Smart City Network. *2020 IEEE International IOT, Electronics and Mechatronics Conference (IEMTRONICS)* **2020**. https://doi.org/10.1109/iemtronics51293.2020.9216386

[42] Loey, M.; Manogaran, G.; Taha, M. H. N.; Khalifa, N. E. M. A hybrid deep transfer learning model with machine learning methods for face mask detection in the era of the COVID-19 pandemic. *Measurement* **2020**, *167*, 108288. https://doi.org/10.1016/j.measurement.2020.108288